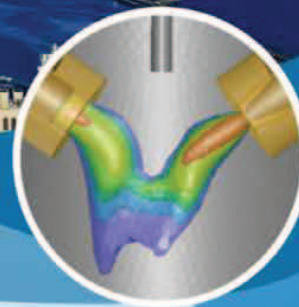
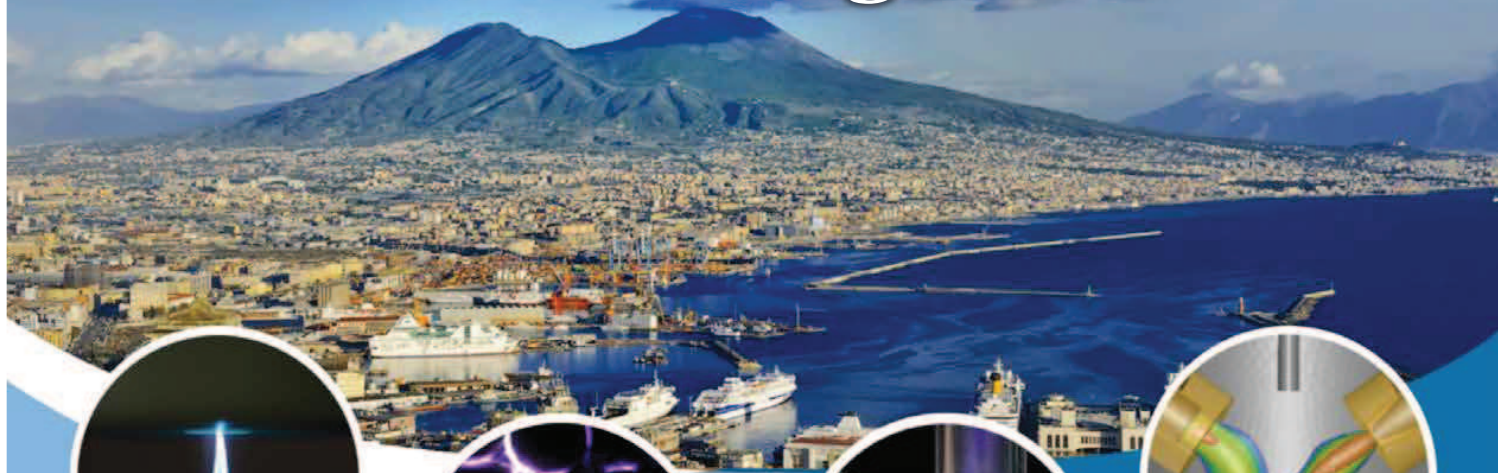


ISPC 24

24TH INTERNATIONAL SYMPOSIUM ON PLASMA CHEMISTRY
NAPLES (ITALY) JUNE 9-14, 2019

Final Program



ALMA MATER STUDIORUM
UNIVERSITÀ DI BOLOGNA

www.ispc24.com



Avenue media[®]

TUESDAY June 11, 2019 (afternoon)			
	ROOM GALATEA	ROOM DIONE	ROOM PERSEIDE
14:00	Chairs Pietro Favia - Rony Snyders	Chairs Anton Nikiforov - Alessandro Patelli	Chairs: Javad Mostaghimi - Gervais Soucy
	<i>Marc Böke</i> Separated effects of plasma species and post-treatment on the properties of barrier layers on polymers O-52 (4)	<i>Bram Wolf</i> Elucidating the role of gas dynamics in the vortex-confined microwave plasma on CO ₂ dissociation efficiency O-56 (2)	<i>Masasya Shigeta</i> To simulate turbulent thermal plasma flows for nanopowder fabrication I-12 (5)
14:15	<i>Annaëlle Demaude</i> Easy synthesis of hybrid hydrophilic-hydrophobic patterned surfaces by atmospheric plasmas O-53 (4)	<i>Georgi Trenchev</i> Atmospheric pressure glow discharge: design improvement based on modelling and experiments O-57 (2)	
14:30	<i>Huidong Hou</i> Effect of Precursor Chemistry on the microstructure of Ba(Mg _{1/3} Ta _{2/3})O ₃ during Hybrid Suspension/Solution Precursor Plasma Spraying O-54 (4)	<i>Françoise Massines</i> Dual frequency DBDs or how to design an atmospheric pressure plasma for surface treatment I-11 (2)	<i>Vittorio Colombo</i> Design-oriented modelling for the synthesis of Cu nanoparticles by a RF thermal plasma: impact of quenching solutions, radiative losses and thermophoresis O-60 (5)
14:45	<i>Shota Nunomura</i> Defect generation and annihilation in hydrogenated amorphous silicon during plasma treatment O-55 (4)		<i>Yasunori Tanaka</i> Effect of Alternating Gas Injection on Temperature Fields in Reaction Chamber using Inductively Coupled Thermal Plasmas for Nanoparticle Synthesis O-61 (5)
15:00	<i>Maria Adriana Creatore</i> Plasma-assisted atomic layer deposition of highly conductive HfN _x layers I-10 (4)	<i>Javad Mostaghimi</i> Advantages of the New Conical Torch for ICP Spectrometry O-58 (2)	<i>Alexander Ustimenko</i> Plasma Treatment of Biomedical waste O-62 (5)
15:15		<i>Efe Kemaneci</i> A zero-dimensional modelling of a coaxial surface wave discharge in oxygen diluted with hexamethyldisiloxane for the deposition of SiO _x films O-59 (2)	<i>Tae-Hee Kim</i> Reproduction of cosmic dust analogues by non-equilibrium condensation in triple DC thermal plasma jet system O-63 (5)
15:30	Refreshment break (30 min)		
	ROOM GALATEA		
16:00	Chair: Romolo Laurita		
	3 min poster pitches - Session II		
	POSTER AREA		
16:45	Parallel poster sessions (1-2-4-7-8)		
19:00			

Topic 5: Thermal plasma fundamentals and applications

ROOM PERSEIDE

Chairs: Javad Mostaghimi - Gervais Soucy

I-12	<i>To simulate turbulent thermal plasma flows for nanopowder fabrication</i> <u>Masaya Shigeta</u>
O-60	<i>Design-oriented modelling for the synthesis of Cu nanoparticles by a RF thermal plasma: impact of quenching solutions, radiative losses and thermophoresis</i> <u>Vittorio Colombo</u> , Simone Bianconi, Marco Boselli, Matteo Gherardi
O-61	<i>Effect of Alternating Gas Injection on Temperature Fields in Reaction Chamber using Inductively Coupled Thermal Plasmas for Nanoparticle Synthesis</i> <u>Yasunori Tanaka</u> , Kotaro Shimizu, Kazuki Onda, Keita Akashi, Yoshihiko Uesugi, Tatsuo Ishijima, Shiori Sueyasu, Shu Watanabe, Keitaro Nakamura
O-62	<i>Plasma Treatment of Biomedical waste</i> <u>Alexander Ustimenko</u> , George Paskalov, Vladimir Messerle, Alfred Mosse
O-63	<i>Reproduction of cosmic dust analogues by non-equilibrium condensation in triple DC thermal plasma jet system</i> <u>Tae-Hee Kim</u> , Jeong-Hwan Oh, Minseok Kim, Yong Hee Lee, Seung-Hyun Hong, Sooseok Choi

3 MIN POSTER PITCHES – SESSION 2

ROOM GALATEA

Chair: Romolo Laurita

P2-70	<i>A multi-jet Plasma Gun equipped with branching device for the treatment of liquids</i> <u>Alina Bisag</u> , Eric Robert, Romolo Laurita, Matteo Gherardi, Jean-Michel Pouvesle, Vittorio Colombo.
P2-72	<i>Subsurface ferroelectric water provokes a controlled protein adsorption</i> <u>Ezgi Bulbul</u> , Dirk Hegemann
P2-100	<i>Selective Destruction toward A-375 Human Melanoma Cells by Atmospheric Pressure Plasma Jet Treatments</i> <u>Saitong Muneekaew</u> , Meng-Jiy Wang
P2-110	<i>Drug introduction into cells using direct exposure of gas-liquid interfacial plasmas</i> <u>Ryosuke Honda</u> , Shota Sasaki, Keisuke Takashima, Makoto Kanzaki, Takehiko Sato, Toshiro Kaneko
P2-122	<i>Atmospheric Pressure Argon Plasma Jet Assisted Copolymerization of Sulfobetaine Methacrylate and Acrylic Acid for Anti-fouling Application</i> <u>Yueh-Han Huang</u> , Meng-Jiy Wang

Plasma Treatment of Biomedical Waste

V.E. Messerle^{1,2}, A.L. Mosse^{3,4}, A.B. Ustimenko^{4*}, G. Paskalov, O.A. Lavrichshev⁴

¹ Combustion Problems Institute, Almaty, Kazakhstan

² Institute of Thermophysics of SB RAS, Novosibirsk, Russia

³ A.V. Luikov Heat and Mass Transfer Institute, NAS of Belarus, Minsk, Belarus

⁴ Plasmatechnics R&D LLP, Institute of Experimental and Theoretical Physics, al-Farabi Kazakh National University, Almaty, Kazakhstan

⁵ Plasma Microsystem LLC, Los Angeles, CA USA

Abstract: This report presents the results of thermodynamic analysis and experiments on gasification of biomedical waste in plasma reactor. A comparison between the experiment and the calculations showed a good agreement. According to the results of investigations of the waste plasma gasification, no harmful impurities were detected. From the waste organic and mineral mass, respectively, synthesis gas having heat of combustion from 3,510 to 5,664 kJ/kg and a neutral slag were obtained.

Keywords: Biomedical waste, plasma, processing, numerical simulation, experiment.

1. Introduction

Biomedical waste (BMW) occupies a special place among hazardous carbon-containing wastes. Until recently, the problem of BMW utilization was not given much attention because of small volumes of produced BMW in comparison with other types of waste. The BMW includes food waste, paper, wood, textiles, leather, rubber, various types of plastics, glass, metal, ceramics, used therapeutic medicines, including radioactive elements, as well as various medical and chemical ingredients. Any kind of waste containing infectious (or potentially infectious) materials is referred to BMW [1]. The increasing volumes of accumulated BMW represent a serious danger to humans and the environment. To recycle such waste, special technologies must be used. According to the treatment and technologies studies of medical wastes, about 59–60% of them are treated through incineration, 37–20% by steam sterilization (autoclaving), and 4–5% by other treatment methods (landfilling, microwaving, plasma pyrolysis). Healthcare waste incineration has been the major technique used worldwide for disposing materials referred to BMW. Incineration is an engineering process designed to treat healthcare waste by means of thermal decomposition via thermal oxidation at high temperatures between 900 and 1200°C destroying the organic fraction of the waste. However, the incineration process has a potential risk to human health due to formation of highly toxic dioxins, benzo(a)pyrene and furans. One of the promising technologies for BMW processing is plasma gasification [2-6]. Bases for BMW plasma utilization is high-temperature pyrolysis and gasification processes, which, as a result of chemical and physical transformations, lead to destruction and decomposition of both organic and inorganic compounds in the waste. In the process of plasma gasification at temperatures up to 3,000 K all materials, even highly resistant cytotoxic and cytostatic drugs, are destroyed

forming simple stable substances [2]. It is one of the main advantages of BMW plasma gasification.

In this report we present the results of a thermodynamic analysis of BMW plasma treatment process and the description of the plasma installation used for this purpose. The results of experiments on plasma gasification of BMW with production of synthesis gas and neutral slag are presented. The results of calculations and experiments are compared confirming technical feasibility and energy efficiency of air-plasma BMW gasification.

2. Thermodynamic simulation

The BMWs used in this research were bony tissues (bones of animal origin). Chemical composition of the bone tissues (BT) is as follows, wt.%: C - 9.0, H - 2.21, O - 1.99, N - 4, S - 1, P - 16.02, CaCO₃ - 65.78.

To carry out the thermodynamic calculations, the TERRA code was used [7]. It was developed for computations of high-temperature processes and has its own database of thermochemical properties for more than 3,000 chemical agents for a temperature range from 300 to 6,000 K. The database contains thermochemical properties of ionized components and electron gas, which are taken into account in thermodynamic calculations. The calculations were performed for temperatures up to 3,000 K and pressure of 0.1 MPa for the compositions of the technological mixtures shown in Table 1. Scenario 1 models a dry BT plasma processing and Scenario 2 – wet BT processing.

Table 1. Compositions of the technological mixtures.

Scenario	Waste, kg	Air, kg	Steam, kg	Mass ratios (waste/oxidant), kg/kg
1	10	5	-	2
2	10	1	0.5	10*; 20**

* - mass ratio waste / air; ** - mass ratio waste / steam

Figures 1 and 2 show the dependence of the concentration of gaseous components on the temperature of BT processing (variant 1). The concentration of the synthesis gas (CO + H₂) increases with temperature to a maximum value of 53.4 vol.% (28.7 vol.% of CO, 24.7 vol.% of H₂) at T = 1,300 K, with the concentration of methane (CH₄) rising to 0.01 vol.% and that of oxidizing carbon dioxide (CO₂) not exceeding 2.46 vol.% and steam (H₂O) - 3.72 vol.% (Fig. 1). On further increase in the temperature, the concentration of the synthesis gas does not practically vary, whereas that of the oxidizers decreases slightly. The concentration of the ballasting nitrogen (N₂) remains constant in the entire temperature range and is equal to 40.4 vol.%. At a temperature above 2,150 K compounds of calcium, phosphorus, and sulfur appear in the gaseous phase (Fig. 2). The maximum concentration of the phosphorus monoxide (PO) is 0.52 vol.%, of phosphorus oxide (PO₂) is 0.02 vol.%, of atomic phosphorus (P) is 0.01 vol.%, of calcium (Ca) is 1.49 vol.%, of calcium hydroxides CaOH is 0.51 vol.% and of CaO₂H₂ is 0.17 vol.% at 3,000 K.

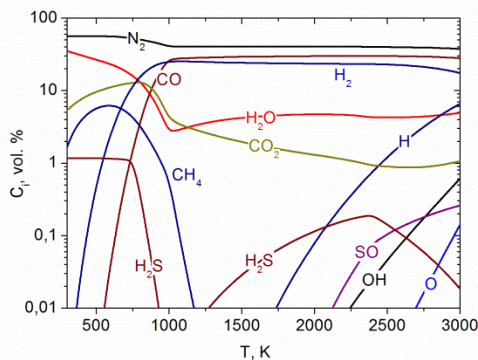


Fig. 1. Equilibrium composition of organic part of the gaseous phase versus temperature in the BT plasma processing (variant 1).

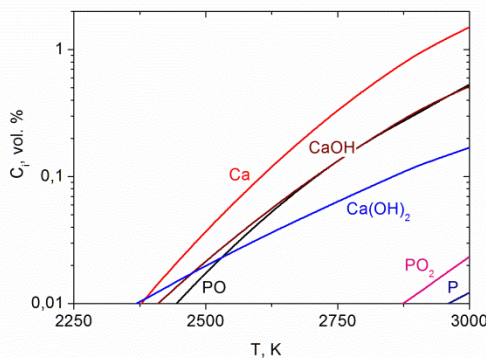


Fig. 2. Equilibrium composition of mineral part of the gaseous phase versus temperature in the BT plasma processing (variant 1).

Figure 3 and 4 show variations in the concentration of gaseous components as a function of temperature of BT processing (variant 2). The concentration of the synthesis

gas increases with temperature to a maximum of 84.9 vol.% (38.1 vol.% of CO, 46.8 vol.% of H₂) at T = 1,300 K (Fig. 3). The concentration of methane (CH₄) comes to 0.2 vol.% and that of oxidizer (CO₂ + H₂O) does not exceed 0.25 vol.%. On further increase in the temperature, the concentration of the synthesis gas remains practically constant, whereas that of the oxidizer increases. The concentration of the ballasting nitrogen (N₂) remains constant in the entire temperature range and is equal to 14.7 vol.%. Compounds of calcium, phosphorus, and sulfur appear in the gaseous phase at a temperature above 1,600 K (Fig. 4). The concentration of phosphorus anhydride (P₂O₃) passes through a maximum of 19.18 vol.% at T = 2,350 K, of molecular phosphorus (P₂) - 0.56 vol.% at 2,150 K, of phosphorus sulfide (PS) - 0.22 vol.% at 2,750 K, of atomic phosphorus (P) - 0.13 vol.% at 2,850 K, of phosphorus monoxide - 2.14 vol.%, of phosphorus oxide - 0.04 vol.%, of calcium - 1.2 vol.%, of calcium hydroxides CaOH - 0.69 vol.% and that of CaOH₂ - 0.12 vol.% at 3,000 K.

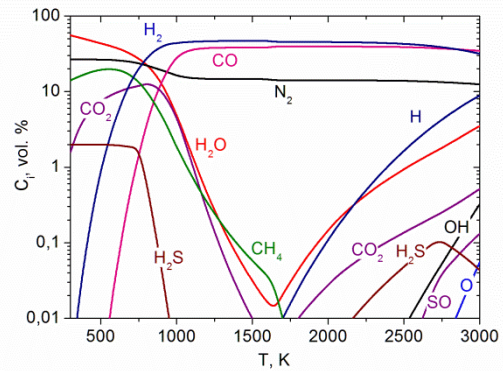


Fig. 3. Equilibrium composition of organic part of the gaseous phase versus temperature in the BT plasma processing (variant 2).

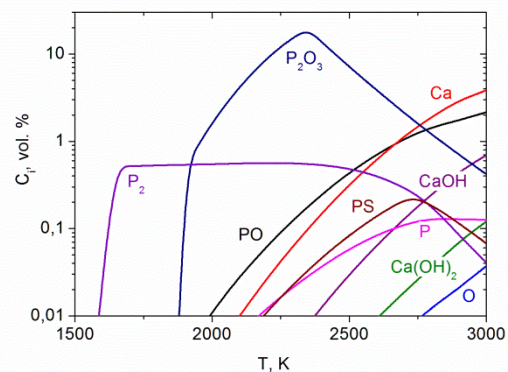


Fig. 4. Equilibrium composition of mineral part of the gaseous phase versus temperature in the BT plasma processing (variant 2).

Figures 5 and 6 show the dependence of concentration of condensed components on the temperature of the process. It is seen from the figures that carbon is entirely converted

into a gaseous phase at a temperature above 1,050 K for variant 1 (Fig. 5) and at 1,600 K for variant 2 (Fig. 6), whereas tricalcium phosphate ($\text{Ca}_3\text{P}_2\text{O}_8$) is in the condensed phase up to the temperature of 3,000 K for both variants. Calcium oxide (CaO) also preserves the condensed phase up to $T = 3,000$ K. Calcium sulfide (CaS) remains in the condensed state up to $T = 2,350$ K for variant 1 (Fig. 5) and 2,700 K for variant 2 (Fig. 6).

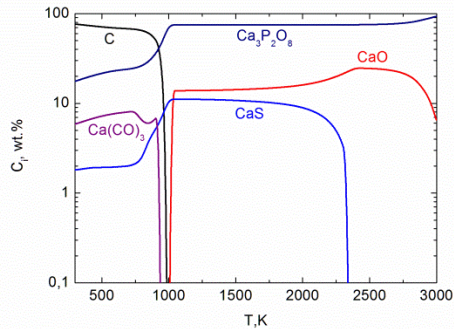


Fig. 5. Temperature dependence of concentration of condensed phase compounds in the BT plasma processing (variant 1).

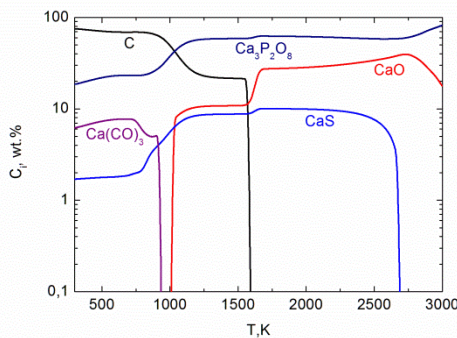


Fig. 6. Temperature dependence of concentration of condensed phase compounds in the BT plasma processing (variant 2).

An addition of steam to the system does not cause a qualitative change in the behavior of the main components of the gaseous and condensed phases and only affects the concentration of hydrogen in the synthesis gas. Thus, processing of the BT composed of organic materials mainly yields a synthesis gas with the content of combustible components 53.4–84.9 vol.%, with the mineral part not containing carbon and mainly represented by stable compounds – tricalcium phosphate and calcium oxide.

The specific power inputs BMW processing increase with temperature in its entire range for the both variants used in the calculations. The temperature dependences of the power inputs at air and steam BMW gasification are quantitatively similar. In the range of optimal temperatures of BMW processing ($T = 1,200 - 1,650$ K), the specific power inputs vary within 0.6 – 1.1 kW h/kg for variants 1 and 2, respectively.

The degree of carbon gasification X_C is determined from the carbon content in the solid residue. In particular, X_C is calculated using the following expression: $X_C = (C_{ini} - C_{fin})/C_{ini} \cdot 100\%$, where C_{ini} is the initial amount of carbon in the waste, and C_{fin} is the final amount of carbon in the solid residue. The degree of carbon gasification amounts to 100 % at a temperature 1,200 K for the both variants. It means that carbon is completely transformed into the gaseous phase forming CO at these temperatures (Figs. 1, 3, 5, 6).

3. Experimental

The experimental study of BMW gasification was carried out on an experimental setup, the primary components of which were a DC plasma torch with rated power of 70 kW and a plasma reactor whose output in terms of BMW was up to 30 kg/hour. Apart from the reactor 2 with the plasma torch 3 (Fig. 7), the experimental facility included a power supply system, a control system of the plasma torch, gas and water supply systems for the reactor with the plasma torch, and a purification system for off-gases 6. The experimental facility was equipped with an extraction system 9 of gaseous products of the BMW gasification process for performing subsequent analysis of the products. Condensed products of the gasification process were accumulated at the bottom of the reactor and analyzed after sampling. The height of the Reactor for BT gasification is 0.33 m, the length is 0.22 m, its width is 0.22 m, and the thickness of the refractory-lining with firebricks is 0.04 m. The reaction volume of the reactor was 0.016 m³. The mass of charged wastes was up to 7 kg.

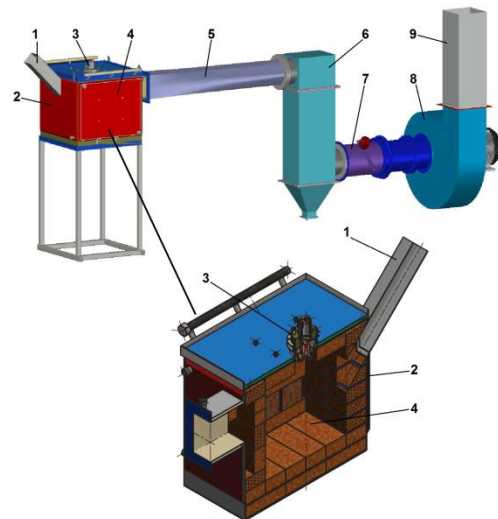


Fig. 7. Scheme of the experimental facility for BMW plasma gasification: 1 – an inlet for loading briquetted BMW into the reactor, 2 – a plasma reactor, 3 – an electric-arc direct current plasma torch, 4 – a BMW gasification zone, 5 – an off-gas cooling unit, 6 – a gas-cleaning unit with a bag filter, 7 – an exhaust gas tube with a system for gas sampling and temperature measurement, 8 – an exhaust fan, 9 – an exhaust tube. In the experiments, the BT consumption G_{BT} varied within 5.4–10.8 kg/h. The amount of the plasma-forming

air G_g reached 3.6 kg/h. The ratio G_{BT}/G_g is equal to 1.5–3. BT of mass 5–7 kg packed up into bags or boxes are placed in the chamber of the furnace, after which the loading hatch is closed. Under the action of the air plasma torch the mean-mass temperature in the chamber rises up to 1,800 K, the organic part of the BT is gasified, whereas the inorganic part is melted. The synthesis gas obtained is extracted through the cleaning and cooling system and is continuously removed from the installation. The melted mineral part of the wastes is taken out of the reactor when it is stopped. The effluent gas at the outlet from the plasma reactor is shown in Table 2. The total concentration of the synthesis gas ($\text{CO} + \text{H}_2$) was 69.6 vol.%, which agrees well with the results of calculation. According to the calculation, the gas output at 1,800 K was 53.4 vol.% (variant 1) and 85.2 vol.% (variant 2). The difference between the experiment and calculations does not exceed 23%.

Table 2. Comparison of modelling and experimental results on BT plasma processing.

Method	CO, vol. %	H ₂ , vol. %	N ₂ , vol. %	S, vol. %	Ca, wt. %	P, wt. %	O, wt. %	X _C , %	Q _{sp} , kWh/kg
Experiment	63.4	6.2	29.6	0.15	54.6	12.9	32	79.3	4.0
Calculation (variant 1)	28.7	24.7	40.4	0.2	40.9	18.7	40.4	100	1.7

X-ray phase analysis showed that the sample taken in the reactor after the experiment was composed of, wt.%: Ca – 54.6, P – 12.9, O – 32, in the form of oxides, CaO – 76.4 and P₂O₃ – 22.9. The content of carbon in the sample was equal to 2.9 wt.%. It corresponds to carbon gasification degree 79.3 %. The difference between the experimental and calculated data does not exceed 21%. Analysis of the condensed products collected from the filter downstream of the reactor showed the following content of elements, wt.%: Ca – 41.5, P – 14.1, O – 33, and S – 1.1. All these elements are present in the sample in the form of oxides (wt.%): CaO – 67, P₂O₃ – 25, and SO₂ – 1. These results for the stable nonvolatile components in the condensed phase (CaO + P₂O₃) correlate with the results of calculations: (CaO + Ca₃P₂O₈) – 89.5 wt.% (variant 1) and 89.9 wt.% (variant 2). The difference between the experimentally obtained and calculated concentrations of calcium and phosphorous oxides does not exceed 3%.

The experimental data on the specific power inputs for the BT processing in the reactor vary from 3.5 to 4.6 kW·h/kg. Such a significant discrepancy between the calculated and experimental values of specific power inputs for the process is attributed to the fact that in the thermodynamic calculations we determine the maximum possible energy expenditures in an isolated thermodynamic system without accounting for the heat exchange with the environment. In practice, both the plasma reactor itself and plasma torch have considerable thermal losses into the surrounding medium with cooling water.

4. Conclusions

The thermodynamic calculations have shown that the maximum synthesis gas yield in the BMW plasma gasification was achieved at a temperature not higher than 1,600 K.

Experiments on plasma-air gasification of BT showed that total concentration of the synthesis gas was 69.6 vol.%, respectively. Carbon gasification degree reached 79.3 and the specific power inputs range within 3.5 - 4.6 kW·h/kg.

Based on the results of thermodynamic calculations and gas and X-ray analyses, no harmful impurities were found in the gaseous and condensed products of the plasma gasification process of BMW. From the organic and mineral mass of BMW, respectively, synthesis gas and a neutral slag were obtained.

The obtained characteristics of the BMW plasma gasification process in various gasifying agents can be used in developing and constructing a plasma facility.

5. Acknowledgements

This work was supported by the Ministry of Education and Science of the Republic of Kazakhstan (projects BR05236507, BR05236498, AP05130731 and AP05130031).

6. References

- [1] Z. Singh, R. Bhalwar, J. Jayaram, V.W. Tilak. An Introduction to Essentials of Bio-Medical Waste Management. MJAFI, 57 (2), 144-147 (2001).
- [2] F. Fabry, Ch. Rehmert, V.-J. Rohani, L. Fulcheri. Waste Gasification by Thermal Plasma: A Review. Waste and Biomass Valorization. Springer, VAN GODEWIJCKSTRAAT 30, 3311 GZ DORDRECHT, NETHERLANDS, 4 (3), 421-439 (2013).
- [3] I.B. Matveev, S.I. Serbin, N.V. Washchilenko. New Combined-Cycle Gas Turbine System for Plasma-Assisted Disposal of Sewage Sludge. IEEE Trans. Plasma Sci. 44 (12), 3100-3104 (2017).
- [4] V.E. Messerle, A.L. Mosse, A.B. Ustimenko. Processing of biomedical waste in plasma gasifier. Waste Management. 79, 791-799 (2018).
- [5] A.V. Surov, S.D. Popov, V.E. Popov, D.I. Subbotina, E.O. Serba, V.A. Spodobin, Gh.V. Nakonechny, A.V. Pavlov. Multi-gas AC plasma torches for gasification of organic substances. Fuel, 203, 1007-1014 (2017).
- [6] Q. Zhang, L. Dor, D. Fenigshtein, W. Yang, W. Blasiak. Gasification of Municipal Solid Waste in the Plasma Gasification Melting Process. Appl. Energ. 90 (1), 106-112 (2012).
- [7] M. Gorokhovski, E.I. Karpenko, F.C. Lockwood, V.E. Messerle, B.G. Trusov, A.B. Ustimenko. Plasma Technologies for Solid Fuels: Experiment and Theory. J. Energy Inst., 78 (4), 157-171 (2005).